COLOR Online B&W in Print

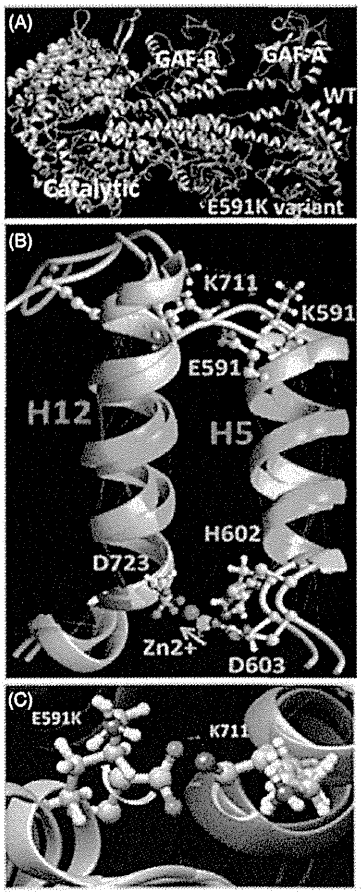

FIGURE 4. Atomic model of a conformational change in the structure of PDE6C caused by the p.E591K mutation. The structure of the mutant variant was obtained by 10 ns–simulated annealing at 37 °C. (A) A general view of the PDE6C dimer (WT) superimposed with the p.E591K mutant subunit is shown. The GAF-A, GAF-B, and catalytic domains are labeled. (B) In the model, the residue conformation and metal ion location in the catalytic site are changed by the p.E591K mutation. Two alpha-helices formed by residues 707–729 (H12, left) and 589–601 (H5, right) are associated with the changes caused by the p.E591K mutation. The image of the two helices is rotated by 180° relative to the image shown at C panel. The locations of hydrophobic residues are shown in green. The movement of the same Zn^{2+} atom is shown by cyan and magenta spheres for the PDE6C catalytic domain and for the same area of the p.E591K mutant variant, respectively. Conformations of residues 602, 603, and 723 forming a binding site for a divalent Zn^{2+} cation are shown. The subunits of PDE6C structure and the superimposed p.E591K mutant variant are shown in beige, light cyan, or light purple, respectively. (C) Local conformation changes in the vicinity of residue K711 are caused by the p.E591K mutation. Yellow arrows show the direction of movement for the respective residue.

p.E591K mutation might reduce PDE activity and thereby disturb the closure of the cGMP-gated ion channel in the cone outer segment membrane, resulting in the loss of hyperpolarization in the cone photoreceptors and leading to ACHM.

Clinical phenotypes of *PDE6C* mutations range from early-onset cone dystrophy to incomplete or complete ACHM.[12,14,31,33] Most ACHM patients with *PDE6C* mutations exhibit normal retinal appearance or only minor macular changes.[12,14,31,33] There have been no reports describing typical macular atrophy in patients with *PDE6C* mutations, although macular atrophy has been reported in patients with *CNGB3* mutations.[6] Moreover, in cases of ACHM due to *CNGB3*, *CNGA3*, or *PDE6C* mutation, some patients exhibit a progressive clinical course, and the progression of ACHM showed a strong association with age.[9,34] Indeed, there is a report that disruption of the retinal pigment epithelium cell layer, which characterizes the end stage of ACHM, was present only in patients over 40 years of age.[34] In our cases, patient IV-1 showed marked macular atrophy since at least 15 years of age.[16] In contrast, patient IV-2 showed only mild macular atrophy at 26 years of age, and he did not have remarkable macular changes until the age of 18.[16] Despite little change or slight worsening of the central scotomas in visual field testing, each patient, IV-1 and IV-2, showed more conspicuous and progressive macular changes at 30 years and 26 years than at 15 years and 18 years, respectively.[16]

The novel *PDE6C* mutation (p.E591K) in a homozygous state could explain part of the phenotypes in our cases, ACHM and slowly progressive disease course. However, it was insufficient to explain the phenotypic differences between the two patients. Our investigation of genetic background clarified there were other potentially relevant mutations or variants in the family (SupplementaryTable S1). Interestingly, those included known disease-causing mutations, *OPN1SW* (p.G79R) and *RHO* (p.T193M), which reportedly cause congenital tritan color vision deficiencies or autosomal dominant retinitis pigmentosa, respectively.[26,27] *OPN1SW* (p.G79R) and *RHO* (p.T193M) were each heterozygous in the father and in patient IV-1. The father (III-1) exhibited blue-yellow color vision deficiencies and no S-cone response in the spectral ERG (Figure 3), but he did not exhibit retinitis pigmentosa; this phenotypic combination indicated congenital tritan deficiencies. Patient IV-1, who had complete ACHM, exhibited normal rod ERG responses.[16] Also functional analysis of *RHO* mutations indicates that the p.T193M was probably an unexplained or misdiagnosed mutation, and incorrectly associated with RP.[35] Taken together, these results suggest that the *RHO* mutation (p.T193M) was non-pathogenic, reversing the earlier report of pathogenesis of retinitis pigmentosa.[26] Based on our whole-exome analysis, we could hypothetically explain the phenotypic difference between the two affected siblings (IV-1 and IV-2). Specifically, we hypothesized that the homozygous *PDE6C* mutation (p.E591K) might underlie incomplete ACHM (patient IV-2), whereas loss of function of OPN1SW in addition to

the *PDE6C* mutation might give rise to complete ACHM (patient IV-1). Additionally, we hypothesized that the heterozygous *OPN1SW* mutation might affect the function of mutated PDE6C, acting as a modifier allele because both OPN1SW and PDE6C proteins are co-expressed in the S-cone outer segments. Baraas and colleagues reported that a heterozygous *OPN1SW* mutation (p.R283Q) causes a significant disruption of the cone mosaic in the foveal area using adaptive optics retinal imaging; their findings indicated that a subset of individuals with congenital tritan deficiencies could exhibit progressive foveal cone loss.[36] Further clinical and genetic studies in individuals with congenital tritan deficiencies will be necessary to confirm our hypotheses.

In conclusion, using whole-exome sequencing, we identified a novel *PDE6C* mutation in two cases of ACHM, one complete the other incomplete, with macular atrophy. The different phenotypes (complete and incomplete ACHM) between the siblings might be explained by a "direct effect" or "possible modifier effect" of the *OPN1SW* mutation (p.G79R) found in the case of complete ACHM. Our data extended the phenotypic spectrum of retinal disorders caused by *PDE6C* mutations and provided new clinical and genetic information.

ACKNOWLEDGEMENTS

We thank the patients and their families for participation in this study.

The authors wish to acknowledge RIKEN GeNAS for the sequencing of the exome-enriched libraries using Illumina HiSeq2000.

DECLARATION OF INTEREST

The authors report no conflicts of interest. The authors alone are responsible for the content and writing of the paper.

This work was supported by grants to T.I. from the Ministry of Health, Labor and Welfare of Japan [13803661], to M.A. and T.H. from the Ministry of Education, Culture, Sports, Science and Technology of Japan [Grant-in-Aid for Scientific Research C, 25462744 and 25462738], and to M.F. from the Research Grant for RIKEN Omics Science Center MEXT.

REFERENCES

1. Kohl S, Hamel C. Clinical utility gene card for achromatopsia – update 2013. Eur J Hum Genet 2013;00:1–000.
2. Voke-Fletcher J. Congenital rod monochromatism in a brother and sister. Mod Probl Ophthalmol 1978;19:236–237.
3. Andreasson S, Tornqvist K. Electroretinograms in patients with achromatopsia. Acta Ophthalmol (Copenh) 1991;69: 711–716.
4. Alpern M, Falls HF, Lee GB. The enigma of typical total monochromacy. Am J Ophthalmol 1960;50:996–1012.
5. Harrison R, Hoefnagel D, Hayward JN. Congenital total color blindness: a clincopathological report. Arch Ophthalmol 1960;64:685–692.
6. Khan NW, Wissinger B, Kohl S, et al. *CNGB3* achromatopsia with progressive loss of residual cone function and impaired rod-mediated function. Invest Ophthalmol Vis Sci 2007;48:3864–3871.
7. Kohl S, Coppieters F, Meire F, et al. A nonsense mutation in *PDE6H* causes autosomal-recessive incomplete achromatopsia. Am J Hum Genet 2012;91:527–532.
8. Sundin OH, Yang JM, Li Y, et al. Genetic basis of total colourblindness among the Pingelapese islanders. Nat Genet 2000;25:289–293.
9. Kohl S, Baumann B, Broghammer M, et al. Mutations in the *CNGB3* gene encoding the beta-subunit of the cone photoreceptor cGMP-gated channel are responsible for achromatopsia (*ACHM3*) linked to chromosome 8q21. Hum Mol Genet 2000;9:2107–2116.
10. Aligianis IA, Forshew T, Johnson S, et al. Mapping of a novel locus for achromatopsia (*ACHM4*) to 1p and identification of a germline mutation in the alpha subunit of cone transducin (*GNAT2*). J Med Genet 2002;39:656–660.
11. Kohl S, Marx T, Giddings I, et al. Total colourblindness is caused by mutations in the gene encoding the alpha-subunit of the cone photoreceptor cGMP-gated cation channel. Nat Genet 1998;19:257–259.
12. Thiadens AA, den Hollander AI, Roosing S, et al. Homozygosity mapping reveals *PDE6C* mutations in patients with early-onset cone photoreceptor disorders. Am J Hum Genet 2009;85:240–247.
13. Thiadens AA, Roosing S, Collin RW, et al. Comprehensive analysis of the achromatopsia genes *CNGA3* and *CNGB3* in progressive cone dystrophy. Ophthalmology 2010;117: 825–830, e821.
14. Grau T, Artemyev NO, Rosenberg T, et al. Decreased catalytic activity and altered activation properties of PDE6C mutants associated with autosomal recessive achromatopsia. Hum Mol Genet 2011;20:719–730.
15. Thiadens AA, Slingerland NW, Roosing S, et al. Genetic etiology and clinical consequences of complete and incomplete achromatopsia. Ophthalmology 2009;116:1984–1989 e1981.
16. Hayashi T, Kozaki K, Kitahara K, et al. Clinical heterogeneity between two Japanese siblings with congenital achromatopsia. Vis Neurosci 2004;21:413–420.
17. Hayashi T, Gekka T, Goto-Omoto S, et al. Novel *NR2E3* mutations (R104Q, R334G) associated with a mild form of enhanced S-cone syndrome demonstrate compound heterozygosity. Ophthalmology 2005;112: 2115–2122.
18. Katagiri S, Yoshitake K, Akahori M, et al. Whole-exome sequencing identifies a novel *ALMS1* mutation (p.Q2051X) in two Japanese brothers with Alstrom syndrome. Mol Vis 2013;19:2393–2406.
19. Katagiri S, Hayashi T, Yoshitake K, et al. Novel *C8orf37* mutations in patients with early-onset retinal dystrophy, macular atrophy, cataracts, and high myopia. Ophthalmic Genet 2014;[redacted]:1–8.
20. Katagiri S, Akahori M, Sergeev Y, et al. Whole exome analysis identifies frequent *CNGA1* mutations in Japanese population with autosomal recessive retinitis pigmentosa. PLoS One 2014;9:e108721.

21. Krieger E, Nabuurs SB, Vriend G. Homology modeling. Methods Biochem Anal 2003;44:509–523.
22. Pettersen EF, Goddard TD, Huang CC, et al. UCSF Chimera – a visualization system for exploratory research and analysis. J Comput Chem 2004;25:1605–1612.
23. Verriest G, Van Laethem J, Uvijls A. A new assessment of the normal ranges of the Farnsworth-Munsell 100-hue test scores. Am J Ophthalmol 1982;93:635–642.
24. Mantyjarvi M. Normal test scores in the Farnsworth-Munsell 100 hue test. Doc Ophthalmol 2001;102:73–80.
25. Hayashi T, Gekka T, Omoto S, et al. Dominant optic atrophy caused by a novel *OPA1* splice site mutation (IVS20+1G–>A) associated with intron retention. Ophthalmic Res 2005;37:214–224.
26. Cideciyan AV, Hood DC, Huang Y, et al. Disease sequence from mutant rhodopsin allele to rod and cone photoreceptor degeneration in man. Proc Natl Acad Sci U S A 1998;95:7103–7108.
27. Weitz CJ, Miyake Y, Shinzato K, et al. Human tritanopia associated with two amino acid substitutions in the blue-sensitive opsin. Am J Hum Genet 1992;50:498–507.
28. Barren B, Gakhar L, Muradov H, et al. Structural basis of phosphodiesterase 6 inhibition by the C-terminal region of the gamma-subunit. EMBO J 2009;28:3613–3622.
29. Hart AW, McKie L, Morgan JE, et al. Genotype-phenotype correlation of mouse pde6b mutations. Invest Ophthalmol Vis Sci 2005;46:3443–3450.
30. Thaung C, West K, Clark BJ, et al. Novel ENU-induced eye mutations in the mouse: models for human eye disease. Hum Mol Genet 2002;11:755–767.
31. Chang B, Grau T, Dangel S, et al. A homologous genetic basis of the murine *cpfl1* mutant and human achromatopsia linked to mutations in the *PDE6C* gene. Proc Natl Acad Sci U S A 2009;106:19581–19586.
32. Granovsky AE, Natochin M, McEntaffer RL, et al. Probing domain functions of chimeric PDE6alpha'/PDE5 cGMP-phosphodiesterase. J Biol Chem 1998;273:24485–24490.
33. Huang L, Zhang Q, Li S, et al. Exome sequencing of 47 chinese families with cone-rod dystrophy: mutations in 25 known causative genes. PLoS One 2013;8:e65546.
34. Thiadens AA, Somervuo V, van den Born LI, et al. Progressive loss of cones in achromatopsia: an imaging study using spectral-domain optical coherence tomography. Invest Ophthalmol Vis Sci 2010;51:5952–5957.
35. Rakoczy EP, Kiel C, McKeone R, et al. Analysis of disease-linked rhodopsin mutations based on structure, function, and protein stability calculations. J Mol Biol 2011;405:584–606.
36. Baraas RC, Carroll J, Gunther KL, et al. Adaptive optics retinal imaging reveals S-cone dystrophy in tritan color-vision deficiency. J Opt Soc Am A Opt Image Sci Vis 2007;24:1438–1447.

Supplementary Material Available Online
Supplementary Figure S1
Supplementary Table S1

Association of retinal artery and other inner retinal structures with distribution of tapetal-like reflex in Oguchi's disease

Yu Kato[1,2,3], Kazushige Tsunoda[1,2], Kaoru Fujinami[1,2,4,5], Takeshi Iwata[6], Masamichi Saga[4], Yoshihisa Oguchi[4]

[1]Department of Ophthalmology, National Tokyo Medical Center, Tokyo, Japan

[2]Laboratory of Visual Physiology, National Institute of Sensory Organs, Tokyo, Japan

[3]Department of Ophthalmology, Tokyo Metropolitan Komagome Hospital, Tokyo, Japan

[4]Keio University, School of Medicine, Department of Ophthalmology, Tokyo, Japan

[5]UCL Institute of Ophthalmology, London, UK

[6]Laboratory of Molecular and Cellular Biology, National Institute of Sensory Organs, Tokyo, Japan

Total word count: 3098 words in the main text.

None of the authors has any financial/conflicting interests to disclose.

19 This research was supported by 1) research grants from the Ministry of Health, Labor
20 and Welfare, Japan and 2) Grant-in-Aid for Scientific Research, Japan Society for the
21 Promotion of Science, Japan.

22

23 Address for reprints: Kazushige Tsunoda, Division of Vision Research, National
24 Institute of Sensory Organs, 2-5-1 Higashigaoka, Meguro-ku, Tokyo 152-8902, Japan
25 tel: +81-3-3411-0111, ext. 6615
26 fax: +81-3-3411-0185
27 e-mail: tsunodakazushige@kankakuki.go.jp

28

29 **Keyword:** Oguchi's disease, tapetal-like reflex, Mizuo-Nakamura phenomenon, *SAG*

30 gene, fundus photograph

Purpose: To report novel ophthalmoscopic features of patients with Oguchi's disease, and to describe how they may be related to the unusual tapetal-like fundus appearance.

Methods: Twenty-one eyes of 11 patients who were diagnosed with Oguchi's disease were investigated. Genetic screening of seven cases showed homozygous mutations in the *SAG* gene (c.926delA). The retinal appearance was retrospectively assessed in the fundus photographs, and the optical coherence tomographic (OCT) and fundus autofluorescence (AF) images.

Results: In 11 eyes of 7 patients, clearly demarcated dark regions without tapetal-like reflex were observed in the mid-peripheral retinal regions. In the dark regions, OCT showed lower reflectances in the photoreceptor layer but the AF images had normal reflectances. In 9 eyes of 6 cases, the dark regions were partially demarcated by retinal arteries but not by veins. In 9 eyes of 5 cases, the extent of the dark regions either increased or decreased during the course of the disease process, and these changes were not due to the state of adaptation or a posterior vitreous detachment. In all eyes, the peripheral retinal arteries but not veins had either high or low reflective regions along one side.

Conclusions: Although the alterations of the outer retinal layers are believed to be most responsible for the abnormal tapetal-like reflex in patients with Oguchi's disease,

these ophthalmoscopic features cannot be explained solely by the abnormality of the outer retina. Our findings suggest that the appearance of tapetal-like reflex is strongly affected by alterations of structures in the inner retinal layers.

Financial Disclosure(s): The author(s) have no proprietary or commercial interest in any materials discussed in this article.

Oguchi's disease is an unusual form of congenital stationary night blindness and is characterized by a golden or grayish-white tapetal-like reflex of the fundus.[1] This unusual reflex disappears only after a long period of dark-adaptation.[2] Mutations in the arrestin gene (s-antigen; *SAG*, OMIM 181031)[3] or the rhodopsin kinase gene (g protein-couples receptor kinase 1; *GRK1*, OMIM 180381)[4] have been identified as the causative genes. Most of Japanese patients have mutations in the *SAG* gene.[3,5-7]

Oguchi described the abnormal fundus appearance of the first patient (22-year-old man) in 1907.[1] He reported that the retinal reflex in the periphery appeared finely marbled just as if it was covered by hoarfrost. The degree of abnormality increased gradually toward the periphery. The choroidal vessels could not be observed except in the far periphery. The peripheral retinal vessels appeared much clearer than in the normal retina but the tips of the vessels appeared darkened. The vessels appeared elevated above the background just like the veins of a leaf, and the peripheral vessels had high reflectivity along one side.

These characteristic ophthalmoscopic findings were reported over one hundred years ago, and the origin of unusual fundus reflex has been investigated by various methods; histopathological assessments,[8,9] intraretinal injection of potassium chloride,[10] surgical removal of the vitreous,[11] scanning laser ophthalmoscopy,[12] optical coherence

74 tomography (OCT),[13-16] and adaptive optics scanning light ophthalmoscopy.[15] In spite
75 of all of these studies, the underlying mechanism of the tapetal-like reflex has not been
76 definitively determined.
77 We have carefully examined the fundi of eleven patients with Oguchi's disease, and
78 found that there are ophthalmoscopic features that have not been reported. Our
79 findings suggest that the inner retinal structures including the vitreoretinal interface,
80 retinal nerve fiver layer (RNFL), and retinal arteries contributed to the appearance of
81 tapetal-like reflex. These findings provide important insights on the origin of the
82 unusual fundus reflex in eyes with Oguchi's disease.
83

84 ## Patients and Methods

85 This was a retrospective case series performed at the National Institute of Sensory
86 Organs, Tokyo, Japan and in the Department of Ophthalmology, Keio University, Tokyo,
87 Japan. An informed consent had been received from all of the subjects for the tests
88 after an explanation of the procedures to be used. In addition, permission was obtained
89 to use their medical data for research. The procedures used adhered to the tenets of
90 the Declaration of Helsinki, and approval to perform this study was obtained from the
91 Review Board/Ethics Committee of the National Institute of Sensory Organs and Keio

University.

Twenty-one eyes of 11 patients (4 men and 7 women, age 12 to 79 years) who were diagnosed with Oguchi's disease were studied (**Table**). The left eye of Case 7 was excluded from the analysis because the fundus photographs were of poor quality. In all eyes, the fundus had a diffuse or localized golden tapetal-like reflex which is pathognomonic for Japanese cases of Oguchi's disease. The full-field scotopic ERGs were non-recordable after 30 minutes of dark-adaptation. The mixed rod-cone bright-flash responses had an electronegative shape with reduced a-wave and severely reduced or absent b-wave. The photopic ERGs were normal. These ERG findings are typical of Oguchi's disease. The visual acuity was normal in all of the patients except Case 10 who had untreated senile cataracts.

Genetic analyses were performed in seven cases, and all had the same homozygous mutation in the *SAG* gene (c.926delA), which is frequently found in Japanese patients with Oguchi's disease.[3,5-7]

Photographs of the posterior pole to the equator were taken with fundus cameras (TRC-50X, TRC-50IA, and TRC-50DX type IA; Topcon , Tokyo, Japan), and the characteristic features, such as distribution patterns of tapetal-like reflex and appearance of the retinal vessels, were retrospectively assessed independently by two experienced

ophthalmologists (YK and KT). In cases where the conclusions were different, discussions were held until both examiners agreed.

OCT images were obtained in the light-adapted condition by spectral-domain OCT (Cirrus HD-OCT, version 6.5; Carl Zeiss Meditec, Dublin, CA) and by swept-source OCT (DRI OCT-1 Atlantis; Topcon, Tokyo, Japan) following pupil dilation. Fundus autofluorescence (AF) images were obtained in the light-adapted condition with a confocal scanning laser ophthalmoscope (HRA 2, Heidelberg Engineering, Heidelberg, Germany; excitation light, 488 nm; barrier filter, 500 nm; field of view, 55°) following pupil dilation.

Results

Dark regions demarcated by retinal arteries

Under room-light conditions of the outpatient clinic, a tapetal-like reflex was observed in all of the cases but its distribution was not homogeneous over the entire retina. In 11 eyes of 7 cases, there were clearly demarcated dark regions without a tapetal-like reflex (**Fig. 1, arrows; Table**). These dark regions were located along or posterior to the equator in all 11 eyes. In 9 eyes of 6 cases, the dark regions were partially demarcated by retinal arteries but not by veins (**Fig. 2, arrows**). In the dark regions, the retina

128 appeared slightly depigmented compared to that of normal Japanese individuals. The
129 depigmentation was observed in patients both with and without myopia and did not seem
130 to be associated with myopic changes (Table). Choroidal vessels could be clearly seen
131 only in the dark regions (**Fig. 2**).
132
133 **Optical coherence tomography and fundus autofluorescence imaging**
134 The OCT images showed that the reflectance of the photoreceptor layer was much
135 higher in the region with tapetal-like reflex than in the dark region as previously
136 described (**Fig. 3**). Regions with tapetal-like reflex had higher reflectivity of the
137 photoreceptor inner segment ellipsoid (ISe) line and of the layer of photoreceptor outer
138 segment above the RPE. There were no apparent structural abnormalities in either
139 the inner or outer retinal layers or choroid (**Fig. 3A**). In the AF images, there were no
140 demarcated lesions corresponding to the dark regions in the fundus photograph (**Fig. 3B,**
141 **asterisks**).
142
143 **Expansion and contraction of dark regions**
144 In 9 eyes of 5 cases (Cases 1, 2, 3, 4, 11), fundus photographs had been serially taken
145 over several years, and we compared the changes in the tapetal-like reflex. In the right

eye of Case 1, the dark region in the superior temporal retina was replaced by the tapetal-like reflex from the periphery that expanded toward the center (**Fig. 4A**). In the left eye of Case 2, the dark region in the nasal retina was replaced by a tapetal-like reflex of the periphery that expanded toward the center, and the dark region was not present at the age 22 years (**Fig. 4B**). In the right eye of Case 3, the region with tapetal-like reflex in the inferior retina was replaced by a dark region that expanded from the center toward the periphery. Thus, the dark regions gradually expanded in these eyes (**Fig. 4C**). In the right eye of Case 1, the regions with and without the tapetal-like reflex interlaced, and the dark regions either expanded or contracted depending on the retinal locations during the follow-up period (**Fig. 4D**). In total, only an expansion of the dark regions was observed in 3 eyes of 2 cases, and only a contraction of the dark regions was observed in 3 eyes of 2 cases. In 3 eyes of 2 cases, both expansion and contraction of the dark regions was observed depending on the retinal locations (**Table**). None of these patients noticed either an improvement or reduction of nyctalopia after the distribution pattern changed.

To exclude the possibility that the changes in distribution of the dark regions were due to the adaptation status, we examined how the borders of dark regions changed during light adaptation in Case 1. Following three hours of dark-adaptation, the tapetal-like

reflex was not detected in the entire retina, the Mizuo-Nakamura phenomenon, but the reflectivity of the retina did not become homogeneous (**Fig. 5A**). After light-adaptation, the tapetal-like reflex reappeared, and the dark regions became clearly visible in the same location. The borders between the regions with and without tapetal-like reflex are indicated by the white arrows in **Figure 5B**. Their locations did not change during the course of the light-adaptation which would indicate that the changes in distribution of the dark regions were not due to the adaptation state.

High and low reflective regions along peripheral arteries

As described by Oguchi in 1907, the peripheral vessels had either high or low reflective regions running along the vessels (**Fig. 6**). We also found that there were other characteristic features in the reflectance of the retinal vessels. The highly reflective regions were observed only along one side of the arteries but not along the veins (**Fig. 6A, arrowheads**). They had the same color as the tapetal-like reflex and appeared different from the strong vascular reflexes commonly observed in children. The highly reflective regions along the arteries disappeared after three hours of dark-adaptation.

The low reflective regions were observed either along one side or both sides of the arteries but not along the veins (**Fig. 6B, arrowheads**). Following three hours of

dark-adaptation, the dark regions became undetectable due to the disappearance of the tapetal-like reflex in the surrounding regions. The highly reflective regions along the retinal arteries were observed in all of the 21 eyes of 11 cases, and those along the retinal veins were observed in only one eye of Case 4 (**Table**). The low reflective regions along arteries were observed in 19 eyes of 10 cases, and those along veins were not observed in any eyes (**Table**).

There were other unusual findings related to the retinal arteries. In the left eye of Case 4, both highly and lowly reflective regions were observed at the same location of a peripheral artery (**Fig. 6C, left**). In the left eye (**Fig. 6C, middle**) and right eye (**Fig. 6C, right**) of Case 3, the dark regions were observed along the peripheral arteries but were slightly separated from the vessels (**arrowheads in Fig. 6C, middle and right**). The same findings were observed in both eyes of Case 4.

Dark regions along retinal nerve fiber layer

In the right eye of Case 4, there was a dark region without tapetal-like reflex which ran parallel to the RNFL bundle (**Fig. 7, left**). Following prolonged dark-adaptation, the tapetal-like reflex decreased, and the border of the dark region completely disappeared (**Fig. 7, middle**). This dark region was not observed in the fundus photographs 3 years

and 6 months later in this eye (**Fig. 7, right**).

Swept-source optic coherence tomography

High-contrast vitreous images were obtained by swept-source OCT from the eyes of Case 1 (**Fig. 8**). The vitreous was homogeneously distributed over the dark regions, and a posterior vitreous detachment could not be observed. There were no apparent abnormalities in the vitreoretinal interface observed along the border between the tapetal-like reflex and dark regions (**Fig. 8, arrows**).

Discussion

We examined the medical records of 11 cases of Oguchi's disease and found funduscopic findings that have not been reported. In the mid-pheripheral region of the fundus, there were clearly demarcated dark regions without tapetal-like reflex where the retina, RPE, and choroid had normal layered structures in the OCT images (**Figs. 1 and 3**). The dark regions were partially demarcated by retinal arteries but not by the veins (**Fig. 2**). The distribution of the dark regions either expanded or contracted during the course of the disease process, and these changes could not be simply explained by the state of adaptation or the presence of a posterior vitreous detachment (**Figs 4 and 5**).

218 The peripheral retinal vessels had either highly or lowly reflective regions, and these
219 were observed only along arteries and not along veins (**Fig. 6**). There was a dark
220 region without tapetal-like reflex, whose location coincided with that of the RNFL bundle
221 (**Fig. 7**).
222 The mechanism causing the tapetal-like reflex has not been definitively determined.
223 The results of histopathological studies suggested the existence of an abnormal layer
224 between the photoreceptor and the RPE and the presence of fuscin bodies in the RPE.[8]
225 The presence of pigment granules in the nerve fiber layer has also been reported in
226 another study.[9] The histopathological investigations, however have not determined the
227 origin of tapetal-like reflex.
228 De Jong et al. suggested that an increase in the concentrations of extracellular K^+
229 produced the tapetal-like reflex because it resembled spreading depression of electric
230 activity in the retina.[10] They suggested that the increased extracellular concentration of
231 potassium was caused by defective Muller cells and led to the tapetal-like reflex in both
232 X-linked retinoschisis and Oguchi's disease. Considering the genetic origin of Oguchi's
233 disease in the outer retina, however the above explanations do not seem reasonable.
234 Kuroda et al. presented a case of Oguchi's disease in which the tapetal-like reflex
235 disappeared following vitrectomy for the treatment of a rhegmatogenous retinal

236 detachment. They concluded that surgical damage to both the inner limiting membrane
237 and Muller cells led to the release of K^+ into the vitreous cavity. This then led to a
238 decrease in the concentration of K^+ in the extracellular space and disappearance of the
239 tapetal-like reflex.[11] However, this phenomenon occurred under very pathological
240 conditions following vitreous surgery and could not explain the changes in the
241 distribution patterns of the dark regions which occurred spontaneously.
242 The results of recent imaging studies have suggested that alterations of the
243 photoreceptor layer is associated with the presence of the tapetal-like reflex. The
244 alterations of the OCT images of the photoreceptor layer corresponded with the changes
245 in the coloration of the fundus, which would suggest that the regions around the
246 photoreceptor outer segments are the sites of the abnormal coloration.[13-15] This is
247 supported by the causative mutation in the *SAG* gene, which encodes S-arrestin, a
248 photoreceptor protein.
249 Using a helium-neon laser (633 nm) scanning laser ophthalmoscope (SLO), Usui et al.
250 found diffuse, fine, white particles in the deep layers of the retina which were not
251 detected in healthy subjects.[12] The appearance of these particles coincided with the
252 appearance of the tapetal-like reflex. They suggested that the particles were located in
253 the outer retina or RPE, and could be the cause of the abnormal fundus appearance in

254 Oguchi's disease.

255 The changes in the reflectance of the rod photoreceptor mosaics in the adaptive optics
256 scanning light ophthalmoscope also suggested that the photoreceptor layer contributed
257 to the tapetal-like reflex.[15]

258 In our cases, the regions without tapetal-like reflex corresponded with the regions of
259 decreased reflectivity in the photoreceptor layer, i.e., layer between ISe and RPE in the
260 OCT images (**Figs. 3A, 8A and 8B**). As in previous studies, the photoreceptor layer is
261 considered to be the most likely origin of the tapetal-like reflex in Oguchi's disease. The
262 results from the AF imaging indicated that there were no local metabolic abnormalities in
263 the retinal pigment epithelium (RPE) in the areas with and without tapetal-like reflex (**Fig.**
264 **3B**).

265 There were, however several findings of the retinal appearance which could not be
266 explained solely by the abnormalities of the photoreceptor layer. The first was the
267 contribution of retinal arteries which demarcate the dark regions without tapetal-like
268 reflex (**Fig. 2**). The second was the highly or lowly reflective regions along the retinal
269 arteries (**Fig. 6**). Third was the region without tapetal-like reflex whose distribution
270 coincided with that of the RNFL bundle (**Fig. 7**). These findings suggest that the inner
271 retinal layers can affect the appearance of the tapetal-like reflex.